Transmission Dosimetry via MAPS-based Event Discrimination in a Therapeutic LINAC

R.P. Hugtenburg[1,2], E. Piastopoulou[1], L. Hancock[3], R. Page[3] and J.J. Velthuis[3]

(1) College of Medicine, Swansea University, Singleton Park, SA2 8PP, Swansea, U.K.
(2) Department of Medical Physics and Clinical Engineering, Abertawe Bro Morgannwg University Health Board, SA2 8QA, Swansea, U.K.
(3) H.H. Wills Physics Laboratory, University of Bristol, BS8 1TL, Bristol, U.K.

Abstract

Transmission dosimetry, which places detectors upstream of the patient is a promising method of dosimetry for intensity modulated radiotherapy (IMRT). Dose predicted downstream of the patient is affected by attenuation and scattering, and changes in the radiation field are difficult to separate from changes in the beam that might indicate a erroneous treatment. Monolithic active pixel sensor (MAPS) technology offers a potentially cost-effective method for measuring the beam profile in a transmission geometry, where MAPS detectors can be made very thin (interacting with less than 1% of photons), while offering high spatial and temporal resolution, and therefore event shape and energy discrimination to identify the therapeutic component of the beam. This study examines event discrimination in the high dose-rate environment associated with therapeutic linear accelerators as a method of distinguishing these components. Monte Carlo modelling of the LINAC and MAPS detector have been used to predict the spectrum of events in the panel, including an evaluation of the occupancy associated with individual LINAC pulses, occurring at rates of up to 40 Hz. It is shown via modelling and experimental measurements that there is sufficiently low occupancy to allow event discrimination, and that there are identifiable signatures associated with the interactions of high-energy therapeutic photons versus contaminant components traversing the detector.

Introduction

In recent years there has been a dramatic increase in the uptake of intensity-modulated radiotherapy (IMRT) in the UK, and globally. There has also been an associated increase in the number and complexity of radiation fields used, as confidence in the practice has grown. Conventional approaches to treatment verification, such as the use of dosimeters placed on the patient, have become a less effective as a means of in vivo dosimetry. Subsequently there has been a reduction in the use of in-vivo dosimetry at many centers, exposing patients to the risk of mistreatment and the potential for wrongly performed treatments to go undetected.

Transit, or portal, dosimetry, where the dose to the patient is predicted from the downstream, portal image, of the radiation source, has recently been adopted at a number of centers, most particular NKI in Amsterdam where data from the technique showed that approximately 1 in 250 treatments had significant errors [1]. With portal imaging the effects of attenuation and scattering of radiation in the patient are difficult to separate from changes in the beam, leading to a high false-positive rate, and the potential obscuration of errors of delivery in certain circumstances.

Transmission dosimetry which places a thin detector system upstream of the patient is a promising alternative, but unless the detector is thin enough, the presence of the detector can affect the quality of the radiation beam. In megavoltage dosimetry, build-up material, of the order of several cm thickness of water-equivalent material, is generally needed to provide charged-particle equilibrium in order to predict dose at depth in the patient. Furthermore, megavoltage photons produce contaminating charged particles, electrons and positrons, in addition to the penetrating, therapeutic photons. Build-up also serves to mitigate the effect of these contaminating charged particles.

Thus far, commercially available systems [2-4] using a variety of dosimetry systems, all employ significant amounts of build-up, reporting attenuation of the order of several mm of plastic material. An alternative approach is the use of monolithic active pixel sensor (MAPS) technology, which offers a potentially cost-effective method for measuring the beam profile in a transmission geometry, but also offers avenues for predicting dose in the absence of, or with limited charged-particle-equilibrium, and in presence of non-therapeutic, charged-particle contamination. In particular, MAPS detectors can be made very thin (interacting with less than 1% of photons), while offering high spatial and temporal resolution, and therefore a means to identify the therapeutic component of the beam. Recent work has shown that MAPS detectors can resolve the sharp penumbrae associated with high-energy photons [5], which enables the accurate determination of the arrangement of the multileaf collimator (MLC) system in real-time [6], while ongoing studies predict the dose to the patient via Monte Carlo modelling and subtraction of the diffuse, contaminating contributions in the beam. Such detectors are still somewhat limited in their size, the typical radiotherapy field being up to 40x40 cm^2 at 100 cm from the target. The detector is placed closer to the target reducing this requirement somewhat, particular compared to transit dosimetry solutions, 3-side buttable, large-scale detectors currently being described [7].

In this work we examine the potential of a MAPS detector system for the use of the spectroscopic capability, i.e. event-shape and energy discrimination, in order to correctly determine the photon fluence, while excluding the effect of contaminating beam components. There are several challenging aspects to this approach, in particular the therapeutic linear accelerators typically deliver dose-rates in excess of 100 mGy/sec, with a pulse-rate of 400-600 Hz and a pulse-structure on the scale on microseconds. This means that, although extremely fast shuttering systems are now being described [8], data through-put, storage and analysis on the scale of GB per-second may ultimately be required.

Methodology

Calculations and measurements were performed for the Achilles MAPS system used in previous studies [5,6]. The device consists of a 4096 x 4096 pixel array of pitch of 14 micron and an active area of 5.73 x 5.73 cm^2. The detector is positioned at a point 55 cm from the X-ray target and therefore projects to cover a field of approximately 10x10 cm^2 at the patient plane (100 cm from target), which would however only encompasses a fraction of standard radiotherapy treatments. The Achilles can theoretically operate at a frame-rates of up to 100 Hz, however in order to obtain single-pulse data, the beam would need to operate at approximately a quarter of the usual dose-rate used in clinical practice.

Monte Carlo modelling is an established method for determining the spectrum of particles generated by the LINAC. The Monte Carlo code BEAMnrc [9] has been used to create lists of the properties of the particles, or phase-space data, leaving the LINAC due to a single pulse of radiation. By calculating the energy deposition in a regular phantom for standard dosimetric conditions, the conversion between the number of electrons hitting the target in a single pulse was determined to be $8x10^{11}$ electrons.

As it is not feasible to run an completely analogue calculation for this number of histories and a variance reduction method, uniform bremsstrahlung splitting was used to reduce the number of source electrons by a factor of 1000. In this mode, whenever a bremsstrahlung event is determined to occur, the outgoing photon is resampled with a new energy and trajectory. The resampling procedure has the effect of ensuring that the photons will not strike the detector at the same point and the variance reduction reduces the simulation time by approximately a factor of 40. The calculation was performed on a supercomputing cluster (HPC Wales), taking a total of 200 cpu-hours to complete. Faster methods of calculation could be envisaged, but the method of calculation has the advantage of making no prior assumptions about the profiles of photons and electrons.

The particles obtained as phase-space data were then transported through a model of the detector system using the DOSXYZnrc code that has an efficient coding system for voxel geometries. The energy deposition for a single pulse was subsequently analysed, separating therapeutic photons from contaminating charged particles, in order to evaluate the capability of the detector to discriminate between the particles on a basis of the energy deposition and simple modes of clustering.

The Monte Carlo model employed in the calculations uses a 3x4096x4096 lattice to represent the detector. In particular the light-tight rendering with 12 micron layer of Al, the 2 micron dead-layer, and the 12 micron epitaxial (active) layer are included in the model. The 86 micron bulk layer was not included in the simulations to improve the efficiency, as backscattering from the bulk into the epitaxial layer was shown not to be significant contributor to events.

Energy deposition was recorded in the lower epitaxial layer. As many events involve particles crossing from one pixel into a neighbouring pixel, a simple algorithm was devised to establish whether a pixel was isolated (i.e. surrounded by pixels with zero energy deposition), and if not, to exclude the event or sum the energy of the neighbouring pixels into the event.

Experimental studies were performed exposing the detector system to ^{55}Fe and $^{90}Sr/^{90}Y$ sources, in order to achieve an approximate calibration of the detector and to understand and apply corrections for instrumental broadening. The sources generate clear features that are in a comparable energy range to the predominant modes of interaction associated with the megavoltage X-ray beam, which is the formation and traversal of the detector by fast electrons.

Figure 1 and 2 show the spectra recorded for ^{55}Fe and ^{90}Sr, respectively. For ^{55}Fe, K-alpha emission at 5.9 and K-beta emission at 6.5 keV produce a single peak at an ADC unit value of 65 with an FWHM of 35, and can be considered to be approximately monoenergetic. The predominant emission from $^{90}Sr/^{90}Y$ are beta rays with a maximum of 2.28 MeV and therefore exhibits a peak associated with the Landau minimum or minimal ionising density threshold of the particles at 41 ADC, with a FWHM of 23. Assuming linearity the peak position corresponds to an energy of 3.7 keV. The Landau minimum in the stopping power is 349.5 eV/micron for electrons and positrons in silicon, occuring at a kinetic energy of approximately 1.25 MeV, and corresponds to the deposition of 4.2 keV for the particle traversing a 12 micron sensitive layer.

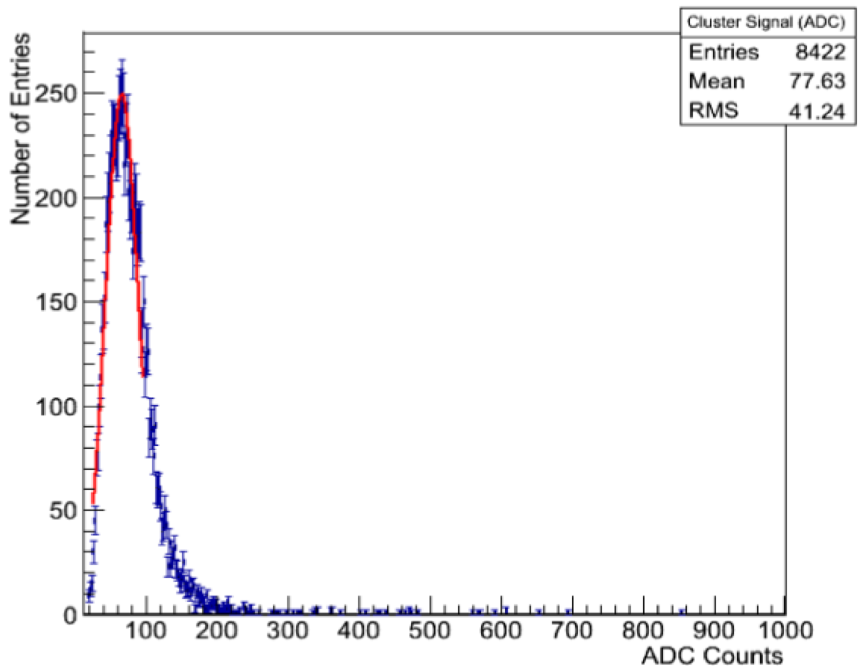

Figure 1. Spectrum obtained with the Achilles MAPS system for ^{55}Fe photon source with principal emission at 5.9 keV corresponding to K-alpha emission occuring upon disintegration.

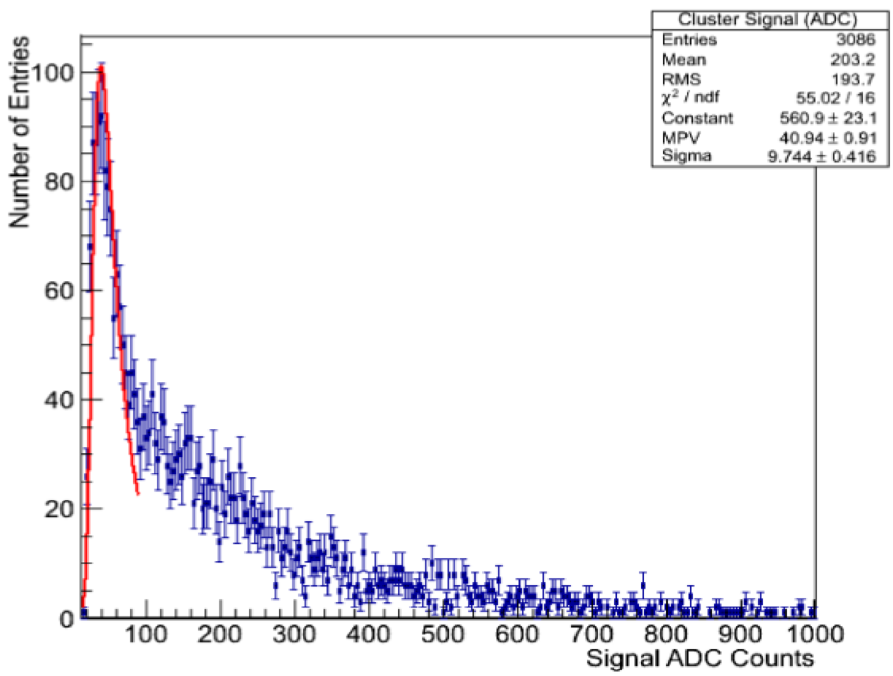

Figure 2. Spectrum obtained with the Achilles MAPS system for a $^{90}Sr/^{90}Y$ β- source. The peak occuring at 3.7 keV is associated with the minimum ionising density threshold for β- particles of kinetic energy, 1.25 MeV.

The Monte Carlo modelling was compared to measurements performed with the Achilles on a SL15 linear accelerator running at low dose-rate of 10 MU/minute. 20 Frames were accumulated and spectra were generated from pixels lying within the open-field field, and outside the field, and therefore exposed to a much lower radiation intensity, shown from previous studies to consist predominately of contaminating electrons.

Results

Figure 3 shows the Monte Carlo calculated event spectra for photon and photon and electron components combined from a single pulse from a 6 MV Elekta Precis LINAC, extracted from the central portion of a 5x5 cm^2 beam. The occupancy, i.e. the fraction of pixels with energy deposition, was found to be appropriately 24%, therefore there was a small but observable probability of multiple events occurring in some pixels. The spectra were broadened to a resolution of ΔE = 1.35 keV (FWHM of 3.2 keV) obtained for the ^{55}Fe exposures, including adding pixels found to have zero energy deposition, utilising comparable spread; noise in empty pixels can be assumed to be comparable in resolution to monoenergetic features at the low-energy limit of the detector. Using the simplistic clustering algorithm, 9.5% of pixels were able to be identified as non-coalesced events in the central 1833x1833 region of the detector corresponding to uniform field of the 5x5 field, while 37% of pixels were found to be empty. The clustering method is satisfactory for Monte Carlo generated data, however the model is somewhat limited in that stochastic noise will be present in empty pixels and does not include the effect of charge sharing, which has the effect of smearing events across neighbouring pixels.

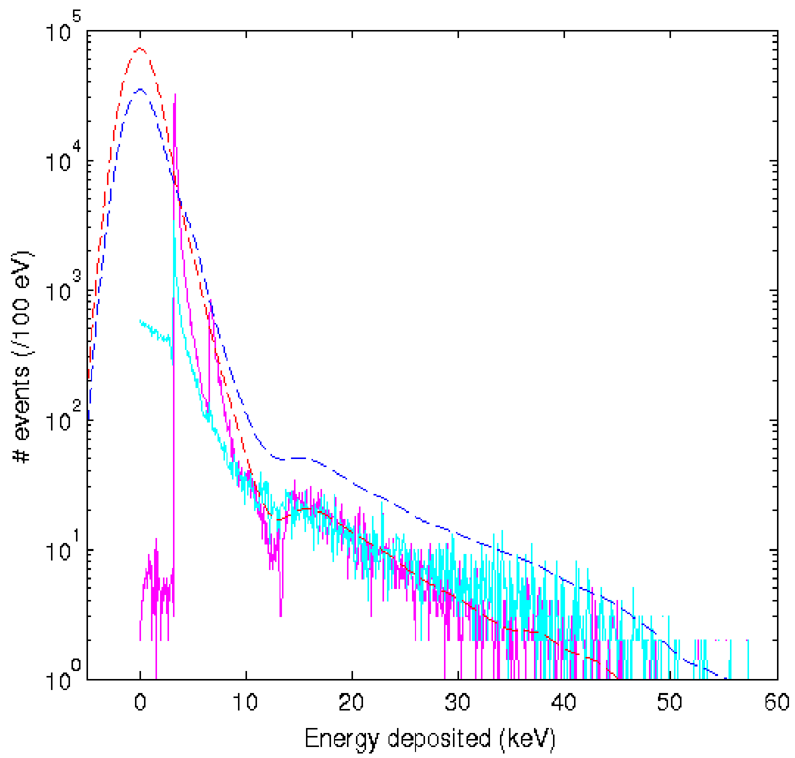

Figure 3. Monte Carlo calculated spectra for all particles (upper solid line) and and contaminating charged particle component (lower solid line) for a single pulse from a therapeutic linac consisting of 8×10^{11} initial electrons at the target. The spectra were smoothed with a Gaussian of ΔE = 1.35 keV, derived from the measurements in the ^{55}Fe 5.9 keV source. Noise was added to pixels containing zero energy to simulate the effect of stochastic noise in the detector and the figure is offset to show this effect below the mean pedestal value.

In the spectra it can be seen that photons are dominate the energy deposition at both low-energy and high-energy limits, the former associated with Compton electrons or pair production interactions occuring in the detector active volume, the latter associated with interactions occuring in the light-tight and dead layers, generating high-angle electrons and positrons, compared with contaminant charged-particles that are generated further upstream.

Figure 4 shows the spectrum obtained from the Achilles detector in the central (open-field) portion of the beam versus the spectrum obtained for regions outside of the beam. Standard procedures are used for the analyse, that include dead-pixel, dark-field pedestal removal and sophisticated event-clustering techniques. Such methods are challenging at the level of occupancy associated with single pulses, and as a consequence the spectra are not as feature-rich as those obtained by Monte Carlo, and predicted at the resolution suggested by low dose-rate sources. In particular charge-sharing between pixels is the predominant effect associated with the loss of resolution at such high occupancy. The differences between the spectra do however appear to follow the overall changes in shape of the spectra obtained from Monte Carlo expected for photon and electron dominated regions.

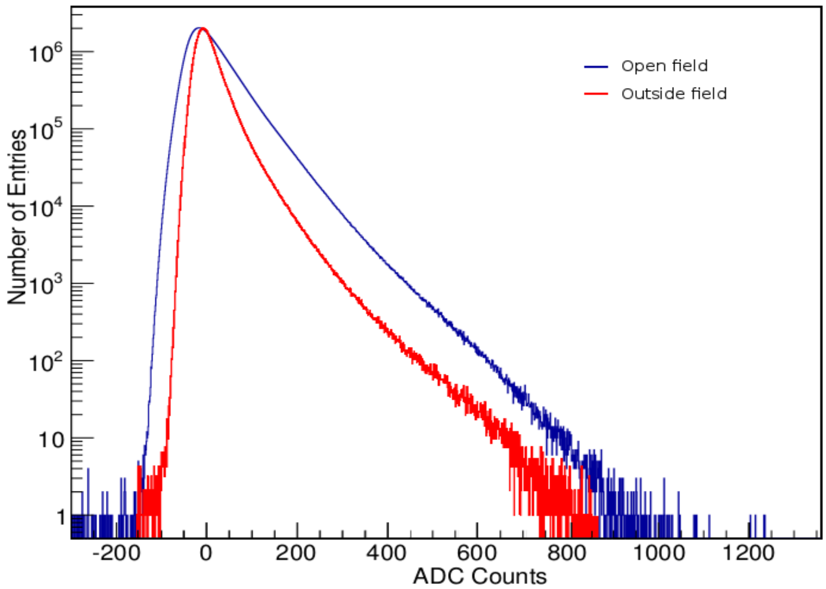

Figure 4. Spectra measured with the Achilles MAPS system for a series of 20 pulses from a Elekta SL15 therapeutic linear accelerator operating at 10 MU s^{-1}, a sufficiently low dose-rate to enable pulse-by-pulse recovery by the device. The open field contains a mixture of photons and contaminating charged particles, while the outside of the field contains predominantly the contaminant radiation due to scattering processes in the head an intervening air.

Conclusions

It has been shown that there is, in principle, a sufficiently low occupancy associated with a single LINAC pulse to allow event discrimination and that there are identifiable signatures associated with the interactions of high energy therapeutic photons in the panel that can assist in discriminating the therapeutic component from contaminating components, principally electrons generated in the head and intervening air.

The high dose associated with a single pulse is a challenging environment for the detector with occupancy at a sufficiently high to level to observe loss of resolution due to difficulties in applying clustering algorithms due to the effects of charge sharing between pixels. Although the Achilles MAP is able to operate at 100 Hz, this is not sufficiently rapid to handle pulse-rates of 400 Hz or more typically used in radiotherapy treatments. A new generation of MAPS detectors promise MHz frame-rates [8] may solve these issues in the near future.

Acknowledgements

The work is supported by the Elizabeth Blackwell Institute for Healthcare Research.

References

[1] M. Wendling, J. Robert, W. Louwe, L. McDermott, J. Sonke, M. van Herk and B. Mijnheer, *Med. Phys.* **2006** ; 33 , 259

[2] M.K. Islam B.D. Norrlinger, J.R. Smale, R.K. Heaton, D. Galbraith, C. Fan and D.A. Jaffray, *Med. Phys.* **2009** ; 36 , 5420

[3] B. Poppe, C. Thieke, D. Beyer, R. Kollhoff, A. Djouguela, A. Rühmann, K.C. Willborn and D Harder, *Phys. Med. Biol*. **2006** ; 51, 1237

[4] S. Venkataraman. K.E. Malkoske, M. Jensen, K.D. Nakonechny, G. Asuni. and B.M.C. McCurdy, *Phys. Med. Biol*. **2009** ; 54 , 3173

[5] J.J. Velthuis, R.P. Hugtenburg, D. Cussans, M. Perry, C. Hall, P. Stevens, H. Lawrence and A. McKenzie, *Appl. Radiat. Isotop.* **2014** ; 83A , 8

[6] R.F. Page, N.L. Abbott, J. Davies, E.L. Dyke, H.J. Randles, J.J. Velthuis, S. Fletcher, S.D. Gregory, C. Hall, A. John, H. Lawrence, P.H. Stevens, R.P. Hugtenburg, V. Tunbridge, *IEEE Trans. Nucl. Sci.* **2014** ; 61 , 74

[7] R. Turchetta, N. Guerrini, and I. Sedgwick, *J. Instrumentation*. 2011; 6, C01099

[8] N. Guerrini and R. Turchetta, G. Van Hoften, R. Henderson, G. McMullan and A R Faruqi, *J. Instrumentation*, **2011** ; 6 , C03003

[9] D.W.O. Rogers, B. Walters and I. Kawrakow, *BEAMnrc Users Manual, NRC Report.* 2006 ; PIRS 509(a) revK